SUPPLEMENTAL MATERIAL

Tomo-seq identifies SOX9 as a key regulator of cardiac fibrosis during ischemic injury

Grégory P.A. Lacraz, MSc, PhD; Jan Philipp Junker, MSc, PhD; Monika M. Gladka, MSc, PhD; Bas Molenaar, MSc; Koen T. Scholman, MSc; Marta Vigil-Garcia, MSc; Danielle Versteeg, BS; Hesther de Ruiter, BS; Marit W. Vermunt, MSc, PhD; Menno P. Creyghton, MSc, PhD; Manon M.H. Huibers, MSc, PhD; Nicolaas de Jonge, MD; Alexander van Oudenaarden, MSc, PhD and Eva van Rooij, MSc, PhD

Supplemental Methods

Ischemia-Reperfusion (IR) injury

Mice were weighed and injected IP with Ketamine/xylazine after which they were ventilated with O_2 containing 1.5–2.5% isoflurane using a micro-ventilator (UMV-03, UNO BV) for anesthesia. The body temperature was maintained at 37°C with a heating pad. After removal of the hair the skin was disinfected with iodine and 10% ethanol and incised on the left of the midline and the heart was accessed via the third intercostal space. A branch of the left anterior descending (LAD) coronary artery was identified and after placing a PE tubing the LAD was ligated with a 7-0 silk suture. Ligation was confirmed by distal cyanosis. Following 1 hr of ischemia, the PE tubing was removed and allowed for the removal of the ligature and subsequent reperfusion. After closing the rib cage with a 5-0 silk suture and the skin with a wound clip, the animals were disconnected from the ventilator and placed unrestrained on a nose cone with 100% oxygen in a warm recovery cage until fully ambulatory, at which point the oxygen was turned off. To alleviate pain or distress, buprenorphine was injected subcutaneously as analgesic (0.05–0.1 mg/kg for mice), given once at completion of surgery. Sham animals underwent an identical operation without induction of the infarct. At the indicated time points after ischemia reperfusion or sham surgery, the animals were killed by an overdose of isoflurane followed by cervical dislocation and tissues were snap-frozen or collected in 4% paraformaldehyde for subsequent analysis.

Tomo-seq

Tomo-seq experiments were performed as described elsewhere. [1] In short, 2.5 mm wide portions of cardiac mouse tissue spanning from the infarct towards the remote region of the left ventricular anterior wall were embedded in tissue freezing medium, frozen on dry ice, and

cryosectioned into 48 slices of 80 μm thickness. We extracted RNA from individual slices and prepared barcoded Illumina sequencing libraries according to the CEL-seq protocol.[2] Paired-end reads obtained by Illumina sequencing were aligned to the transcriptome using BWA.[3] The 5' mate of each pair was used for mapping, discarding all reads that mapped equally well to multiple loci. The 3' mate was used for barcode information. Read counts were normalized to the same number of total reads per section. Tomo-seq data analysis was performed in MATLAB (MathWorks) using custom-written code. For data analysis we used an expression cut-off of >4 reads in >1 section. In differential expression analysis (Figure 1C), we determined the boundary between remote and infarcted zone based on the spatial partitioning detected by pairwise comparison of sections across all genes in one biological replicate (Figure 1B). For the infarcted zone, we used sections 1-26, and for the remote zone we used sections 29-47. The border zone (sections 27-29) was omitted in order to reduce ambiguity in assignment of sections to zones. We then compared the sections within and outside the infarcted zone and assessed statistical significance with Wilcoxon rank sum test. For this analysis, each section was considered as an independent measurement. Furthermore, filtering was applied for genes that showed at least a two-fold expression difference between remote and infarcted zone. For this analysis, the mean expression levels for each gene in the two zones was calculated. Concerning the hierarchical clustering, expression traces of the genes that passed the differential expression filter in Figure 1C were used for analysis. The data was standardized by *Z*-score normalization (along rows of data) so that the mean expression is zero and the standard deviation is 1 in order to remove differences in expression level between genes. Euclidean distance was used as distance metric. The assignment of genes to clusters I-III (Figure 1D) was determined manually considering the similarity in gene expression pattern across the ischemic heart.

In situ hybridization

ISH probe constructs were generated by PCR amplification of partial coding sequence from cDNA of mouse and human heart tissue, and subsequent ligation into either pSPT18 or pSPT19 vectors (Roche). Primers used for partial coding sequence amplification can be found in Supplemental Table 7 online. Probe plasmids were linearized and riboprobes were transcribed from linearized template in the presence of digoxigenin-11-UTP. Mouse hearts were fixed in formaldehyde overnight, and dehydrated stepwise into ethanol. Dehydrated hearts were incubated in xylene for 2 hrs and overnight in paraffin at 55°C. Hearts were embedded in paraffin blocks, which were solidified at room temperature. Hearts were sectioned transversally using a microtome (Leica) and the sections (10 μm thick) were adhered to Starfrost slides. Paraffin was dissolved in xylene and slides were rehydrated stepwise in ethanol. The slides were prepared for hybridization by the following incubations: 0.2 M HCl for 15 min; 30 μg/ml Proteinase K for 15/20 min for mouse/human slides at 37°C. Proteinase K was stopped by rinsing the slides in 0.2% glycine. The slides were post-fixed for 10 min in 4% PFA, then in acetic anhydride 5 min, and washed in SSC buffer. Slides were prehybridized in hybridization buffer for 1 hr at 65°C. Probes were diluted in 1 μg/ml hybridization solution and denatured by heating at 95°C followed cooling on ice. Hybridization buffer and probes were placed on the slides and incubated for 24 hrs at 65°C, after which the hybridization buffer was removed and slides were incubated at 65°C in 50% formamide/2× SSC buffer three times for 15 min. Slides were washed in TBS-T followed by maleic acid buffer. Slides were blocked for at least 30 min at room temperature in blocking solution and incubated with 1:1500 anti-DIG-AP in blocking solution for 3–4 hrs at room temperature. Slides were washed in maleid acid, TBS-T and NTM buffers. Probe detection was carried out by incubation in NBT/BCIP substrate for 4–24 hrs in the dark. As soon as a signal could be detected the reaction was stopped by washing

the slides in NTM buffer and demi-water subsequently, after which they were mounted with aquatex.

Pathway and transcription factor binding site enrichment

To investigate whether genes share a similar biological function, we searched for over-representation in the Kyoto Encyclopedia of Genes and Genomes (KEGG) pathway using DAVID.[4] The enriched genes in the KEGG pathway are shown as *p* values corrected for multiple hypothesis testing using the Benjamini-Hochberg method.

Detection of over-represented conserved transcription factor binding sites in the set of genes spatially co-regulated to *Col1a2* was determined using single site analysis in oPOSSUM 3.0 (online software). The enrichment of SOX9 binding sites was determined using the *Z*-score, which uses the normal approximation to the binomial distribution to compare the rate of occurrence of a TFBS in the target set of genes to the expected rate estimated from the pre-computed background set.

Human heart samples

Approval for studies on human tissue samples was obtained from the Medical Ethics Committee of the University Medical Center Utrecht, The Netherlands (12#387). Written informed consent was obtained or in certain cases waived by the ethics committee when obtaining informed consent was not possible due to death of the patient. In this study, we included tissue from the left ventricular free wall of patients with end-stage heart failure secondary to ischemic heart disease. This end-stage heart failure tissue was obtained at explanation of the failing heart during heart transplantation or at autopsy. For each case three areas of the infarcted heart tissue were included; 1) infarct zone, 2) border zone and 3) remote area. For ISH analysis, three patients were included. From these patients the border zone of the

infarcted hearts was used for ISH to verify tomo-seq and real-time PCR analysis. Left ventricular free wall of non-failing donor hearts, that could not be transplanted for technical reasons, were used for comparison. In these cases, neither donor patient histories, nor echocardiography revealed signs of heart disease.

mRNA analysis

Total RNA from the infarct (containing the infarct and the peri-infarct zone) and the remote zone (classified as myocardial tissue unaffected by the IR), or their equivalent tissue fraction from sham operated hearts, or cultured cells was isolated using Trizol reagent (Invitrogen) according to the manufacturer's instructions and quantified by optical density at 260 nm using a Nanodrop 1000 spectrophotometer (Thermoscientific). For quantitative detection of mRNA levels, complementary DNAs were synthesized by using iScript cDNA Synthesis Kit (Bio-Rad). Real-time PCR analysis was carried out in a CFX96 Connect detection system (Bio-Rad) using gene specific primers (provided in Supplemental Table 8 online) and iQ SYBR Green Supermix (Bio-Rad). Reverse transcribed RNA (10 ng) was used as template for each reaction. All reactions were run in duplicate with no template control. The PCR conditions were: 95ºC for 15 min, followed by 40 cycles at 95ºC for 15 s, 60ºC for 30 s and 72ºC for 30 s. Glyceraldehyde 3-phosphate dehydrogenase (*Gapdh*) was used as house-keeping gene.

Histology and immunofluorescence

Heart tissues from C57BL/6 and mutant mice or human patients were embedded either in paraffin after fixation in 4% formalin for two consecutive days, or in OCT after fixation in PLP buffer containing 0.1 M phosphate buffer containing 0.2 M L-lysine, pH 7.4, 2.12 mg/ml NaIO4, and 4% paraformaldehyde overnight, washed in phosphate buffer, and dehydrated in 30% sucrose in phosphate buffer overnight. Hematoxylin and eosin (H&E) and Sirius Red

stains were performed using routine histology protocols. Images were acquired using a Leica DM4000 M (Leica Microsystems) microscope. The Sirius Red-positive area was determined as a percentage of the infarcted area using ImageJ. $SOX9^+$ cells were quantitated in three different fields (magnification × 20) of the fibrotic area 14dpIR (~1300 cells/heart) or the corresponding region in Sham (~850 cells/heart) (n=3 mouse per group). For immunofluorescence staining, paraffin sections were dewaxed in xylene for 5 min, rehydrated in ethanol (2× 5 min in 100% ethanol, 2× 5 min in 96% ethanol, 2× 5 min in 70% ethanol), and rinsed three times with demi water. This was followed by antigen retrieval boiling with citrate buffer for 20 min. Sections were then washed in PBS, incubated for 45 min at room temperature in a blocking solution containing 1% BSA, 0.01% Triton X-100, and 0.01% Tween20, and then incubated overnight at 4℃ with a primary antibody specific for SOX9 (rabbit, 1:250, Millipore #ab5535), type 1 collagen (mouse, 1:500, Abcam #ab6308), alpha-actinin (ACTN2, mouse, 1:400, Sigma #A7732), and TdTomato (goat, 1:1000, Sicgen #AB8181-200). Sections were incubated for 60–90 min at room temperature with species specific secondary antibodies conjugated with Alexa 488 (1:400, Life Technologies #A11001) or Alexa Fluor 568 (1:300, Life Technologies #A10042 and #A11057). Nuclear counterstaining was performed using DAPI prior to mounting (Prolong Gold antifade reagent, Life Technologies #P36934). Images were acquired using a SPE (Leica Microsystems) microscope.

3T3-L1 cell culture

3T3-L1 cells were purchased from ATCC and cultured in Dulbecco's Minimum GlutaMAX (low glucose) (Gibco) supplemented with 10% FBS (Life technologies). Cells were serum-starved for 16 hrs after which they were transfected for 24 hrs with 10 nM *Sox9* siRNA (Thermoscientific) or scrambled siRNA as control, using Lipofectamin 2000 reagent (Invitrogen) in Opti-MEM media (Gibco). TGFβ1 (5 ng/ml; Preprotech) was then added and

the cells were harvested at the indicated time points for RNA extraction and subsequent real-time PCR analysis.

SOX9 animals models

Sox9 (*Sox9*$^{fl/fl}$) mutant mice harboring two *loxP* sites flanking the exons 2–3 [6] were crossed with *Rosa26-CreERT2* mice (*R26*^{CreERT2}) to obtain an inducible *Sox9* loss-of-functional model (*Sox9*$^{fl/+}$;*R26*^{CreERT2}). For lineage tracing studies, mice expressing *CreERT2* under the control of the *Sox9* promoter [7] were bred with the *Rosa26-tdTomato* reporter mouse (*R26R*^{TdT}) to obtain *Sox9*^{CreERT2};*R26R*^{TdT} mice. To induce the CreERT2 protein, *Sox9*$^{fl/+}$;*R26*^{CreERT2} and *Sox9*^{CreERT2};*R26R*^{TdT} mice were injected with Tamoxifen (corn oil/ethanol) intraperitoneally (2 mg per day per mouse) at the day of surgery and 2 and 4 days after injury. Control mice (referred to as *Sox9*$^{fl/+}$;*R26*^{CreERT2} Vehicle) received an equal volume of the vehicle that was used to deliver Tamoxifen. Primers used for genotyping are provided in Supplemental Table 8 online.

FACS analysis

Hearts (left ventricle) were digested by a medium containing 20 µg/ml DNAse I (Worthington Biochemical #LK003172) and 26 U/ml Liberase™ (Roche #5401020001) for 15 min at 37°C. The dissociated single cells were collected by filtration through a 100-µm nylon mesh. Expression of TdTomato was analysed by flow cytometry using a FACSAria III flow cytometer (BD Biosciences) and the FlowJo software (Tree Star).

Western Blotting

Standard Western blot analysis was performed on homogenates from infarcted hearts of *Sox9*$^{fl/+}$;*R26*^{CreERT2} mice using Periostin antibody (Pierce #PA5-34641) and GAPDH (Merck

#mab374) as a loading control. Densitometry of the Western blots was performed using ImageQuant TL Software (GE Healthcare Life Sciences software).

Statistical analysis

Values are presented as mean ± s.e.m. Previous studies were used to predetermine sample size. Statistical analyses between two groups were conducted using the two-tailed unpaired or paired Student's *t*-test or a Mann-Whitney test when the normality assumption was not met. Comparison among groups was performed using a two-way ANOVA with Bonferroni's post-hoc test. Pearson's correlation coefficients were used to calculate gene pair correlation based on gene expression in human samples. KEGG pathways are ranked by their respective *p* value corrected for multiple hypothesis testing using the Benjamini-Hochberg method. *p* value <0.05 was interpreted to denote statistical significance. Prism 6 (GraphPad Software, Inc.) was used for statistical analyses.

Supplemental Tables

Supplemental Table 1. Functional annotation chart of predicted pathways activated 1 dpIR using the list of differentially regulated genes determined by tomo-seq.

KEGG term	Genes	Fold Enrich ment	P-value
Biosynthesis of unsaturated fatty acids	*Acot1, Acot2, Acot9, Hadha, Hsd17b12, Elovl6, Scd2*	3.6	1.7E-1
Fc gamma R-mediated phagocytosis	*Fcgr1, Fcgr2b, Limk1, Rac2, Was, Cfl1, Dock2, Gsn, Hck, Inpp5d, Map2k1, Ncf1, Pak1, Pik3r1, Pla2g6, Arpc5, Ptprc, Asap1, Vasp, Vav1*	2.8	1.7E-3
Leukocyte transendothelial migration	*Rac2, Rock1, Actb, Actn4, Actn1, Cyba, Itga4, Itgal, Itgam, Itgb2, Mmp9, Mapk11, Myl9, Ncf1, Ncf2, Ncf4, Pxn, Pik3r1, Actg1, Thy1, Vcam1, Vasp, Vav1*	2.7	1.6E-3
Hematopoietic cell lineage	*Cd24a, Cd33, Cd44, Cd9, Fcgr1, Csf2ra, Gp1bb, H2-Eb1, Itga4, Itgam, Il1b, Il1r1, Il1r2, Il11, Il4ra, Csf3r*	2.7	2.2E-2
Regulation of actin cytoskeleton	*Fgd3, Iqgap1, Limk1, Nckap1l, Rac2, Rock1, Was, Actb, Actn4, Actn1, Baiap2, Cfl1, Cyfip1, Cyfip2, Diap1, Enah, Fn1, Gsn, Itga4, Itgal, Itgam, Itgax, Itgb2, Map2k1, Myh14, Myh9, Myl9, Pak1, Pak2, Pxn, Pik3r1, Pdgfra, Pdgfa, Arpc5, Actg1, Rras2, Apc, Mylk3, Tmsb4x, Vav1*	2.6	7.9E-6
Adherens junction	*Crebbp, Iqgap1, Rac2, Was, Actb, Actn4, Actn1, Baiap2, Insr, Actg-ps1, Ptpn1, Ptpn6, Snai1, Tgfbr1*	2.6	5.3E-2
Chemokine signaling pathway	*Fgr, Rac2, Rock1, Was, Arrb2, Xcr1, Ccl2, Ccl21a, Ccl3, Ccl4, Ccl6, Ccl7, Ccl9, Ccr1, Ccr8, Cxcl16, Cxcr6, Dock2, Elmo1, Hck, Cxcr2, Map2k1, Ncf1, Nfkbib, Pak1, Pxn, Pik3r1, Plcb1, Ccl27a, Ppbp, Cxcl5, Vav1*	2.5	3.3E-4
Pyrimidine metabolism	*Prim1, Entpd5, Pola1, Pole3, Pold4, Polr1c, Polr3a, Tk1, Rrm1, Txnrd1, Tyms, Umps, Upp1, Uck1, Uck2*	2.2	1.4E-1
Cytokine-cytokine receptor interaction	*Relt, Xcr1, Ccl2, Ccl21a, Ccl3, Ccl4, Ccl6, Ccl7, Ccl9, Ccr1, Ccr8, Cxcl16, Ccr6, Csf2ra, Csf2rb, Csf2rb2, Crlf2, Il1b, Il1r1, Il1r2, Il10ra, Il11, Il15, Il17ra, Il4ra, Il8ra, Pdgfra, Pdgfa, Csf3r, Il2rg, Ccl27a, Ppbp, Cxcl5, Tgfb2, Tgfbr1, Tnfrsf12a*	2.1	2.0E-3
Focal adhesion	*Elk1, Rac2, Rock1, Vwf, Actb, Actn4, Actn1, Diap1, Fn1, Flnc, Itga4, Map2k1, Myl9, Pak1, Pak2, Parva, Pxn, Pik3r1, Pgf, Pdgfra, Pdgfa, Actg-ps1, Mylk3, Tnc, Thbs1, Vasp, Vav1, Zyx*	2.0	1.9E-2

Supplemental Table 2. Functional annotation chart of predicted pathways activated 14 dpIR using the list of differentially regulated genes determined by tomo-seq.

KEGG term	Genes	Fold Enrichment	P-value
Valine, leucine and isoleucine degradation	*Hmgcs2, Hibch, Oxct1, Auh, Acat1, Acaa2, Acadm, Acadsb, Aldh6a1, Dbt, Dld, Ehhadh, Hadh, Ivd, Mccc1, Mccc2, Mcee, Mut, Hibadh, Hadhb, Pcaa*	3.5	1.0E-5
ECM-receptor interaction	*Cd36, Agrn, Comp, Chad, Col1a1, Col1a2, Col3a1, Col4a2, Col5a1, Col5a2, Col6a1, Col6a2, Col11a1, Fn1, Itga11, Itga2b, Itga6, Itgav, Itgb5, Itgb8, Lamc1, Sdc2, Sdc3, Sdc4, Tnc, Tnxb, Thsb1, Thsb2, Thsb3, Thsb4, Vtn*	3.1	7.9E-8
Hypertrophic cardiomyopathy (HCM)	*Serca2, Actc1, Actb, Ace, Cacna1c, Cacna2d1, Cacnb2, Des, Igf1, Itga11, Itga2b, Itga6, Itgav, Itgb5, Itgb6, Itgb8, Lmna, Myh7, Prkaa2, Prkag1, Ryr2, Sgcg, Ttn, Tgfb2, Tgfb3, Tnni3, Tnnt2*	2.5	2.8E-4
Lysosome	*Abca2, Atp6v0b, Atp6v0d1, Atp6ap1, Cd63, Cd68, Gm2a, Asah1, Ap1s1, Ap4s1, Naglu, Arsa, Ctsa, Ctsd, Ctsf, Ctsk, Ctss, Ctsz, Clta, Fuca1, Glb1, Gns, Gba, Gusb, Hexa, Hexb, Lgmn, Lipa, Lamp1, Laptm5, Man2b1, Manba, Neu1, Pla2g15, Ap3s1, Slc11a1, Smpd1*	2.4	6.9E-6
Oxidative phosphorylation	*Atp5b, Atp5j, Atp5f1, Atp5g3, Atp6v0b, Atp6v0d1, Atp6ap1, Ndufa1, Ndufa2, Ndufa4, Ndufa4l2, Ndufa5, Ndufa6, Ndufb3, Ndufb4, Ndufb5, Ndufb6, Ndufab1, Ndufc2, Ndufs1, Ndufs4, Ndufs5, Cox7b, Cox7a2, Atp5l, Atp5g2, Atp5h, Atp5g1, Uqcrh, Uqcrb, Atp5k, Ndufc1, Gm5457, Cox6c, Ndufs3, Sdha, Sdhb, Sdhd, Uqcrc2*	2.3	2.0E-5
Focal adhesion	*Bcl2, Flt4, Rac2, Src, Actb, Actn4, Actn1, Bcar1, Figf, Comp, Chad, Col1a1, Col1a2, Col3a1, Col4a2, Col5a1, Col5a2, Col6a1, Col6a2, Col11a1, Egf, Egfr, Fn1, Flnc, Flna, Flnb, Igf1, Itga11, Itga2b, Itga6, Itgav, Itgb6, Itgb8, Lama4, Lamb2, Lamc1, Mapk3, Myl9, Parva, Pik3cd, Pik3r2, Pip5k1c, Pdgfra, Pdgfrb, Myl12b, Prkcb, Ppp1ca, Tln1, Tnc, Tnxb, Thsb1, Thsb2, Thsb3, Thsb4, Vasp, Vav1, Vtn, Zyx*	2.3	1.4E-7
Dilated cardiomyopathy	*Actc1, Actb, Adcy4, Adcy7, Cacna1c, Cacna2d1, Cacnb2, des, Igf1, Itga11, Itga2b, Itga6, Itgav, Itgb5, Itgb6, Itgb8, Lmna, Pln, Ryr2, Sgcg, Tnt, Tgfb2, Tgfb3, Tpm2, Tnni3, Tnnt2*	2.2	1.3E-3
Alzheimer's disease	*Atp5b, Atp5j, Atp5f1, Atp5g3, Bad, Ndufa1, Ndufa2, Ndufa4, Ndufa4l2, Ndufa5, Ndufa6, Ndufb3, Ndufb4, Ndufb5, Ndufb6, Ndufab1, Ndufc2, Ndufs1, Ndufs4, Ndufs5, App, Apoe, Bace2, Cacna1c, Capn1, Casp9, Cdk5, Cox7b, Cox7a2, Eif2ak3, Gnaq, Itpr1, Lpl, Mapk3, Cycs, Atp5g2, Atp5h, Atp5g1, Uqcrh, Uqcrb, Ndufc1, Gapdh, Gm5457, Cox6c, Ndufs3, Sdha, Sdhb, Sdhd, Serca2, Tnfrsf1a, Uqcrc2*	2.2	2.6E-6
Parkinson's disease	*Atp5b, Atp5j, Atp5f1, Atp5g1, Atp5g2, Atp5g3, Atp5h, Ndufa1, Ndufa2, Ndufa4, Ndufa4l2, Ndufa5, Ndufa6, Ndufb3, Ndufb4, Ndufb5, Ndufb6, Ndufab1, Ndufc2, Ndufs1, Ndufs4, Ndufs5, Casp9, Cox7b, Cox7a2, Cycs, Uqcrb, Uqcrh, Ndufc1, Gm5457, Cox6c, Ndufs3, Slc25a4, Sdha, Sdhb, Sdhd, Uqcrc2, Uchl1, Ube2l6*	2.2	3.2E-5
Huntington's disease	*Atp5b, Atp5j, Atp5f1, Atp5g3, Ndufa1, Ndufa2, Ndufa4, Ndufa4l2, Ndufa5, Ndufa6, Ndufb3, Ndufb4, Ndufb5, Ndufb6, Ndufab1, Ndufc2, Ndufs1, Ndufs4, Ndufs5, Ap2b1, Ap2s1, Casp9, Clta, Cox7b, Cox7a2, Dctn1, Dctn4, Gnaq, Ap2a2,*	2.1	6.5E-6

	Itpr1, Ppargc1a, Polr2f, Cycs, Atp5g2, Atp5h, Atp5g1, Uqcrh, Uqcrb, Ndufc1, Gm5457, Cox6c, Gm7511, Ap2m1, Ndufs3, Hdac1, Slc25a4, Sdha, Sdhb, Sdhd, Tfam, Uqcrc2		
Regulation of actin cytoskeleton	*Cd14, Rras, Iqgap1, Nckap1l, Rac2, Arhgef6, Arhgef1, Arhgef7, Tiam1, Was, Arpc1b, Arpc4, Actb, Actn4, Actn1, Baiap2, Bcar1, Csk, Chrm2, Egf, Egfr, Fgf1, Fgf13, Fgfr1, Fn1, Itga11, Itga2b, Itga6, Itgam, Itgav, Itgb2, Itgb5, Itgb6, Itgb8, Mapk3, Mras, Myh9, Myl9, Pik3cd, Pik3r2, Pip5k1b, Pip5k1c, Pdgfra, Pdgfrb, Myl12b, Arpc2, Gm5637, Ppp1ca, Nras, Slc9a1, Vav1*	1.8	5.5E-4

1

Supplemental Table 3. Functional annotation chart of predicted pathways activated 14 dpIR using the one hundred fifty most similar genes to the cardiac stress gene *Col1a2* determined by tomo-seq.

KEGG term	Genes	Fold Enrichment	P-value
ECM-receptor interaction	*Col1a1, Col1a2, Col3a1, Col5a1, Col5a2, Fn1, Itgb1, Thbs1, Thbs4*	16.9	2.0E-7
TGF-beta signaling pathway	*Dcn, Id2, Id3, Thbs1, Thbs4,Tgfb3*	11.3	5.0E-4
Focal adhesion	*Actn1, Col1a1, Col1a2, Col3a1, Col5a1, Col5a2, Fn1, Igf1, Itgb1, Thbs1, Thbs2, Thbs4*	8.5	1.7E-6
Antigen processing and presentation	*Ctsl, Ctss, H2-Ab1, H2-Eb1, Lgmn*	7.7	5.0E-2

Supplemental Table 4. Functional annotation chart of predicted pathways activated 14 dpIR using the one hundred fifty most similar genes to the cardiac stress gene *Nppa* determined by tomo-seq.

KEGG term	Genes	Fold Enrichment	P-value
Prion diseases	*C1qa, C1qb, Lamc1*	10.9	2.6E-1
Ribosome	*Rpl11, Rps21, Rps14, Rpsa, RplP0, Fau, Rpl37*	10.0	2.7E-3
Hypertrophic cardiomyopathy	*Actb, Itgb5, Lmna, Myh7*	6.1	2.9E-1
ECM-receptor interaction	*Comp, Itgb5, Lamb2, Lamc1*	6.1	3.6E-1
Dilated cardiomyopathy	*Actb, Itgb5, Lmna, Myh7*	5.5	2.5E-1
Focal adhesion	*Actb, Comp, Flna, Itgb5, Lamb2, Lamc1, Rhoa*	4.5	9.2E-2
Tight junction	*Rras, Actb, Myh7, Rhoa*	3.8	4.8E-1

Supplemental Table 5. Functional annotation chart of predicted pathways activated 14 dpIR using the one hundred fifty most similar genes to the cardiac stress gene *Serca2* determined by tomo-seq.

KEGG term	Genes	Fold Enrichment	P-value
Fatty acid elongation in mitochondria	*Acaa2, Hadh, Hadhb*	32.1	1.6E-2
Valine, leucine and isoleucine degradation	*Oxct1, Auh, Acat1, Acaa2, Acadm, Dbt, Dld, Hadh, Ivd, Hibadh, Hadhb*	20.5	6.0E-10
Oxidative phosphorylation	*Atp5b, Atp5j, Atp5f1, Atp5g3, Ndufa2, Ndufa5, Ndufa6, Ndufb3, Ndufb5, Ndufb6, Ndufc2, Ndufs1, Ndufs4, Cox7b, Cox7a2, Atp5h, Uqcrh, Uqcrb, Atp5k, Ndufc1, Cox6c, Ndufs3, Sdha, Sdhb, Sdhd, Uqcrc2*	17.1	1.7E-23
Parkinson's disease	*Atp5b, Atp5j, Atp5f1, Atp5g3, Ndufa2, Ndufa5, Ndufa6, Ndufb3, Ndufb5, Ndufb6, Ndufc2, Ndufs1, Ndufs4, Cox7b, Cox7a2, Atp5h, Uqcrh, Uqcrb, Ndufc1, Cox6c, Ndufs3, Slc25a4, Sdha, Sdhb, Sdhd, Uqcrc2*	16.7	1.5E-23
Alzheimer's disease	*Atp5b, Atp5j, Atp5f1, Atp5g3, Ndufa2, Ndufa5, Ndufa6, Ndufb5, Ndufb6, Ndufc2, Ndufs1, Ndufs4, Cox7b, Cox7a2, Atp5h, Uqcrh, Uqcrb, Ndufc1, Cox6c, Ndufs3, Slc25a4, Sdha, Sdhb, Sdhd, Uqcrc2*	12.2	6.8E-23
Huntington's disease	*Atp5b, Atp5j, Atp5f1, Atp5g3, Ndufa2, Ndufa5, Ndufa6, Ndufb5, Ndufb6, Ndufc2, Ndufs1, Ndufs4, Cox7b, Cox7a2, Atp5h, Uqcrh, Uqcrb, Ndufc1, Cox6c, Ndufs3, Slc25a4, Sdha, Sdhb, Sdhd, Uqcrc2*	12.2	3.1E-20
Fatty acid metabolism	*Acat1, Acaa2, Acsl1, Acadl, Acadm, Hadh, Hadhb*	13.3	6.7E-5
Citrate cycle (TCA cycle)	*Cs, Dlat, Dld, Fh1, Idh2, Mdh1, Pdha1, Sdha, Sdhb, Sdhd, Sucla2*	11.0	1.1E-8
Cardiac muscle contraction	*Serca2, Actc1, Cacna1c, Cox7b, Cox7a2, Uqcrh, Uqcrb, Cox6c, Ryr2, Uqcrc2*	11.0	1.4E-6
PPAR signaling pathway	*Cd36, Acsl1, Acadl, Acadm, Fabp3, Fabp4, Lpl*	7.6	1.5E-3

Supplemental Table 6. Conserved transcription factor binding sites (TFBS) for the set of 30 genes showing the greatest similarity in expressional regulation to *Col1a2* 14 dpIR in mice.

Transcription factor	Class	Family	Target gene hits	*Z*-score
NFATC2	Ig-fold	Rel	28	15.631
RUNX1	Ig-fold	Runt	28	11.582
FOXO3	Winged Helix-Turn-Helix	Forkhead	27	6.786
Nkx2-5	Helix-Turn-Helix	Homeo	28	6.461
YY1	Zinc-coordinating	BetaBetaAlpha-zinc finger	28	5.285
KLF4	Zinc-coordinating	BetaBetaAlpha-zinc finger	25	5.200
SOX17	Other Alpha-Helix	High Mobility Group	28	4.838
SOX9	**Other Alpha-Helix**	**High Mobility Group**	**27**	**4.227**
Arnt::Ahr	Zipper-Type	Helix-Loop-Helix	26	3.659
PRXX2	Helix-Turn-Helix	Homeo	27	3.022
SPI1	Winged Helix-Turn-Helix	Ets	29	2.876
EBF1	Zipper-Type	Helix-Loop-Helix	25	2.842
TBP	Beta-sheet	TATA-binding	26	1.089
ELK1	Winged Helix-Turn-Helix	Ets	25	-2.576
ZEB1	Zinc-coordinating	BetaBetaAlpha-zinc finger	29	-3.273

Results are sorted by *Z*-score for the detected transcription factors regulating ≥25 *Col1a2* co-regulated genes.

Supplemental Table 7. List of primer sequences used to create *in situ* hybridization probes.

Gene	Organism	Sequence
Chchd2	Mus Musculus	Fw SalI_GTCGACCTTATTGGTTGCCCGGTGAG Rv BamH1_GGATCCCAAGGAGGCCAAACACTTCC
Col1a2	Mus Musculus	Fw XbaI_GCTCTAGACCTTGACATTGCACCTCTGG Rv SacI_GCGAGCTCATGAAGAGAGAACCTGGGGC
Fstl1	Mus Musculus	Fw XbaI_GCTCTAGAGACGCCCTCATTGAACTGTC Rv SacI_GCGAGCTCCTCCATGGCGCTTGAAGTAC
Nppa	Mus Musculus	Fw XbaI_GCTCTAGAAGCAAACATCAGATCGTGCC Rv SacI_GCGAGCTCATATGCAGAGTGGGAGAGGC
Nppb	Mus Musculus	Fw XbaI_GCTCTAGAAGGAAATGGCCCAGAGACAG Rv SacI_GCGAGCTCCAAAAGCAGGAAATACGCTATGT
Pln	Mus Musculus	Fw XbaI_GCTCTAGAAGTGCAATACCTCACTCGCT Rv SacI_GCGAGCTCCATGTACACAGCCCTTGAGC
Pmepa1	Mus Musculus	Fw SalI_GCGTCGACCTCTTCCCCTTTCCATCTCC Rv BamH1_GCGGATCCCTCACCAAGCTAGGCACCTC
Serca2	Mus Musculus	Fw XbaI_GCTCTAGAGGTTCGAGGAAGGGGAAGAA Rv SacI_GCGAGCTCTGTGGTAAGTGTGCCTGTCT
Sox9	Mus Musculus	Fw XbaI_GCTCTAGAACATGGAGGACGATTGGGAGA Rv SacI_GCGAGCTCAGGGTGATAGTCTGAGCAGGC
Sparc	Mus Musculus	Fw XbaI_GCTCTAGACATAAGCTCACCGTCCACAAG Rv SacI_GCGAGCTCGCAAGAACCTGAAAGCCCAA
CHCHD2	Homo sapiens	Fw XbaI_GCTCTAGAGCTTAGCTCTTCGGTGGTTG Rv SacI_ GCGAGCTCTTTGCCCAGTCCCAGATTCT
COL1A2	Homo sapiens	Fw XbaI_GCTCTAGACAAGGTTTCCAAGGACCTGC Rv SacI_GCGAGCTCGAAGACCACGAGAACCAGGA
FSTL1	Homo sapiens	Fw XbaI_GCTCTAGACCCCACTCACTACCCTGTTT Rv SacI_GCGAGCTCACATTCAGACTGGTCCACGT
NPPA	Homo sapiens	Fw XbaI_GCTCTAGAGACAGACGTAGGCCAAGAGA Rv_KpnI_GCGGTACCTAATGCATGGGGTGGGAGAG
PMEPA1	Homo sapiens	Fw Sal1_GCGTCGACCTCTTCCCCTTTCCATCTCC Rv Bamh1_GCGGATCCCTCACCAAGCTAGGCACCTC
SERCA2	Homo sapiens	Fw XbaI_GCTCTAGAATGGTGGTTCATTGCTGCTG Rv SacI_GCGAGCTCTGGAGAGGGATCTGGCTACT
SOX9	Homo sapiens	Fw XbaI_GCTCTAGAAGGAAGTCGGTGAAGAACGG Rv SacI_GCGAGCTCCCGTAGCTGCCCGTGTAG
SPARC	Homo sapiens	Fw XbaI_GCTCTAGAAGTACATCGCCCTGGATGAG Rv SacI_GCGAGCTCGTCCGTGCTCCCAAAAGTTT

Supplemental Table 8. List of primer sequences used for real-time and genotyping PCR.

Gene	Organism	Accession number		Sequence
Acta2	Mus Musculus	NM_007392.2	Forward Reverse	ACCCACCCAGAGTGGAGAAG AGCATCATCACCAGCGAAG
Cdrap	Mus Musculus	NM_019394.3	Forward Reverse	GGCCAAGTGGTGTATGTCTTC GCTGCCAGGTCTCCATAGTAAC
Col1a1	Mus Musculus	NM_007742.3	Forward Reverse	AATGCAATGAAGAACTGGACTG CCCTCGACTCCTACATCTTCTG
Col1a2	Mus Musculus	NM_007743.2	Forward Reverse	CAAGGACCTGCTGGTGAAC TGGTCCAACGACTCCTCTC
Col2a1	Mus Musculus	NM_031163.3	Forward Reverse	GCAAAGATGGCTCTAATGGAA GACTTCCAGGGGGACCAA
Col3a1	Mus Musculus	NM_009930.2	Forward Reverse	GATGGCAAAGATGGATCACCTGG GACCCTTTTCTCCTGGGATGC
Col4a1	Mus Musculus	NM_009931.2	Forward Reverse	GAGAGACAGGACCCTTTGGAC GGTCATCTGTTGTCTGACTATGC
Col5a2	Mus Musculus	NM_007737.2	Forward Reverse	GAAAGGCTGGTGATCAAGGT TTTCTCCCCGAGGTCCTAAT
Col8a1	Mus Musculus	NM_007739.2	Forward Reverse	GCCAGCCAAGCCTAAATGT CAGAGTTCAGGGAAATGATGAA
Col11a1	Mus Musculus	NM_007702.2	Forward Reverse	CAGATTGTGACTTAACATCCAAGG CTCGATTATATCCTCAGGTGCAT
Col11a2	Mus Musculus	NM_009926.1	Forward Reverse	CAGCCTAGCAGATGGCAAAT CAGTCCACAATGAGAGTGACAGA
Col16a1	Mus Musculus	NM_028266.5	Forward Reverse	GCATTGCAGGAGAAAATGGT CCATCTTGCCATAACCTGGA
Ctgf	Mus Musculus	NM_010217.2	Forward Reverse	TGACCTGGAGGAAAACATTAAGA AGCCCTGTATGTCTTCACACTG
Dkk3	Mus Musculus	NM_015814.2	Forward Reverse	TGTGTTGTGCCTTCCAAAGA GTTCCCAGGTGATGAGATCC
Ecm1	Mus Musculus	NM_007899.2	Forward Reverse	AAGTGGAAGGGTCCTTAGCAA TCGATGAAGGCCAGTTTCTC
Fbln1	Mus Musculus	NM_010180.2	Forward Reverse	TGCATCAATACAGTGGGCTCT CCAGTCTCACATTCGTCAATATCT
Fbln2	Mus Musculus	NM_007992.2	Forward Reverse	CAGGTGGCCTCTAACACCAT TTGCAGGGTCCATTGTCTTT
Fn1	Mus Musculus	NM_010233.1	Forward Reverse	CCACTGTGGAGTACGTGGTTAG AAGCAATTTTGATGGAATCGAC
Fstl1	Mus Musculus	NM_008047.5	Forward Reverse	CAGCCATCAACATCACCACT ATGAGGGCGTCAACACAGA
Gapdh	Mus Musculus	NM_008084.2	Forward Reverse	TGTCGTGGAGTCTACTGGTG ACACCCATCACAAACATGG
Htra3	Mus Musculus	NM_030127.2	Forward Reverse	TTGCCACGATTGTAATCCAC GGTGTTCTGCAGGGCAAA

Igf1	Mus Musculus	NM_001111276.1	Forward Reverse	CACCTTCACCAGCTCCACCAC CAGTCTCCTCAGATCACAGCTC
Nppa	Mus Musculus	NM_008725.2	Forward Reverse	GGTAGGATTGACAGGATTGGAG GCTTAGGATCTTTTGCGATCTG
Pdgfrl	Mus Musculus	NM_026840.3	Forward Reverse	TGCAGAGACCTCAAAAGGTG CCTGATCTTCCTCCCAGAAA
Serca2	Mus Musculus	NM_009722.3	Forward Reverse	TGGTGATATAGTGGAAATTGCTG GAGTTGTAGACTTGATGGATGTCAA
Sfrp1	Mus Musculus	NM_013834.3	Forward Reverse	GTGGTTCAAGATGTGCTCCA TCAGAGCAGCCAACATGC
Sox9	Mus Musculus	NM_011448.4	Forward Reverse	TATCTTCAAGGCGCTGCAA TCGGTTTTGGGAGTGGTG
Sparc	Mus Musculus	NM_022316.2	Forward Reverse	CCATTGGCGAGTTTGAGAA GTGCACTTGGTGGCAAAGA
Spp1	Mus Musculus	NM_001204201.1	Forward Reverse	CCCGGTGAAAGTGACTGATT TTCTTCAGAGGACACAGCATTC
Tcf4	Mus Musculus	NM_013685.2	Forward Reverse	CATATTTGTGGCCATTGAAGG CAGCTCTTTGTCCGTCCCTA
Tgfb3	Mus Musculus	NM_009368.3	Forward Reverse	CCCTGGACACCAATTACTGC TCAATATAAAGGGGGCGTACA
Thbs2	Mus Musculus	NM_011581.3	Forward Reverse	TCGGACCTCAAGTATGAGTGC TCTAAGAAGGGGTGTTTGCAG
Tmem45a	Mus Musculus	NM_019631.3	Forward Reverse	AACATTATTACGTCGGACAGAGATT AGATAAACTGTTCACCAGCTATACCA
APOE	Homo sapiens	NM_000041.2	Forward Reverse	GGTCGCTTTTGGGATTACCT CATGGTCTCGTCCATCAGC
ATP5G3	Homo sapiens	NM_001689.4	Forward Reverse	GGTGATATTGTAGAAATTGCTGTTG TGACTGGTCAACTCTTAGTGTGGT
COL1A2	Homo sapiens	NM_000089.3	Forward Reverse	TGATGGAAAAGGAGTTGGACTT CAGGTCCTTGGAAACCTTGA
CHCHD2	Homo sapiens	NM_016139.2	Forward Reverse	GCTGAAACAGTGCCGACTT AACTTAGTTATGAGAGCTGATTTTCCA
CRIP1	Homo sapiens	NM_001311.4	Forward Reverse	GCAACAAGGAGGTGTACTTCG CACATTTCTCGCACTTCAGG
DKK3	Homo sapiens	NM_015881.5	Forward Reverse	GAGGACACGCAGCACAAAT TTTGCCAGGTTCACTTCTGA
FBLN2	Homo sapiens	NM_001004019.1	Forward Reverse	CAGGTGGCCTCTAACACCAT TTGCAGGGTCCATTGTCTTT
FSTL1	Homo sapiens	NM_007085.4	Forward Reverse	GCCATCAATATTACAACGTATCCA TCAATGAGAGCATCAACACAGA
FXYD5	Homo sapiens	NM_144779.2	Forward Reverse	TCAGCAGACTCAACTATCATGGA GGGCTGGAGTTCTGTGTAGACT
GAPDH	Homo sapiens	NM_002046.3	Forward Reverse	GGGTCATCATCTCTGCCCC GGTCATGAGTCCTTCCACGA
HTRA3	Homo sapiens	NM_053044.3	Forward Reverse	AGCTACAGAATGGGGACTCCT AGCAACAACACAGGGAGCTT

NDUFA5	Homo sapiens	NM_005000.2	Forward Reverse	GGTGTGCTGAAGAAGACCACT TTGTGTACAATATTCTTAGCCTCTCG
NPPA	Homo sapiens	NM_006172.3	Forward Reverse	CCGTGAGCTTCCTCCTTTTA CCAAATGGTCCAGCAAATTC
PMEPA1	Homo sapiens	NM_020182.3	Forward Reverse	CTGCACGGTCCTTCATCAG TTGCCTGACACTGTGCTCTC
SERCA2	Homo sapiens	NM_001681.3	Forward Reverse	GGTGATATTGTAGAAATTGCTGTTG TGACTGGTCAACTCTTAGTGTGGT
SLC25A3	Homo sapiens	NM_213611.2	Forward Reverse	TCTTGTATAGCAATATGCTTGGAGA GGGCAATGTCAGCAAAGAAT
SOX9	Homo sapiens	NM_000346.3	Forward Reverse	GTACCCGCACTTGCACAAC TCTCGCTCTCGTTCAGAAGTC
Sox9fl	Transgene	Genotyping primers	Forward Reverse	GTCATATTCACGCCCCCATT AGACTCTGGGCAAGCTCTGG
Sox9fl del	Transgene	Genotyping primers	Forward Reverse	TGGTAATGAGTCATACACAGTAC GTCAAGCGACCCATGAACGC
Sox9creERT2	Transgene	Genotyping primers	Forward Reverse	GCGGTCTGGCAGTAAAAACTATC GTGAAACAGCATTGCTGTCACTT
Cre	Transgene	Genotyping primers	Forward Reverse	GAAGCAACTCATCGATTGATTTACG CACTATCCAGGTTACGGATATAGTTC
TdTomato	Transgene	Genotyping primers	Forward Reverse	CTGTTCCTGTACGGCATGG GGCATTAAAGCAGCGTATCC

1

Supplemental Figure 1

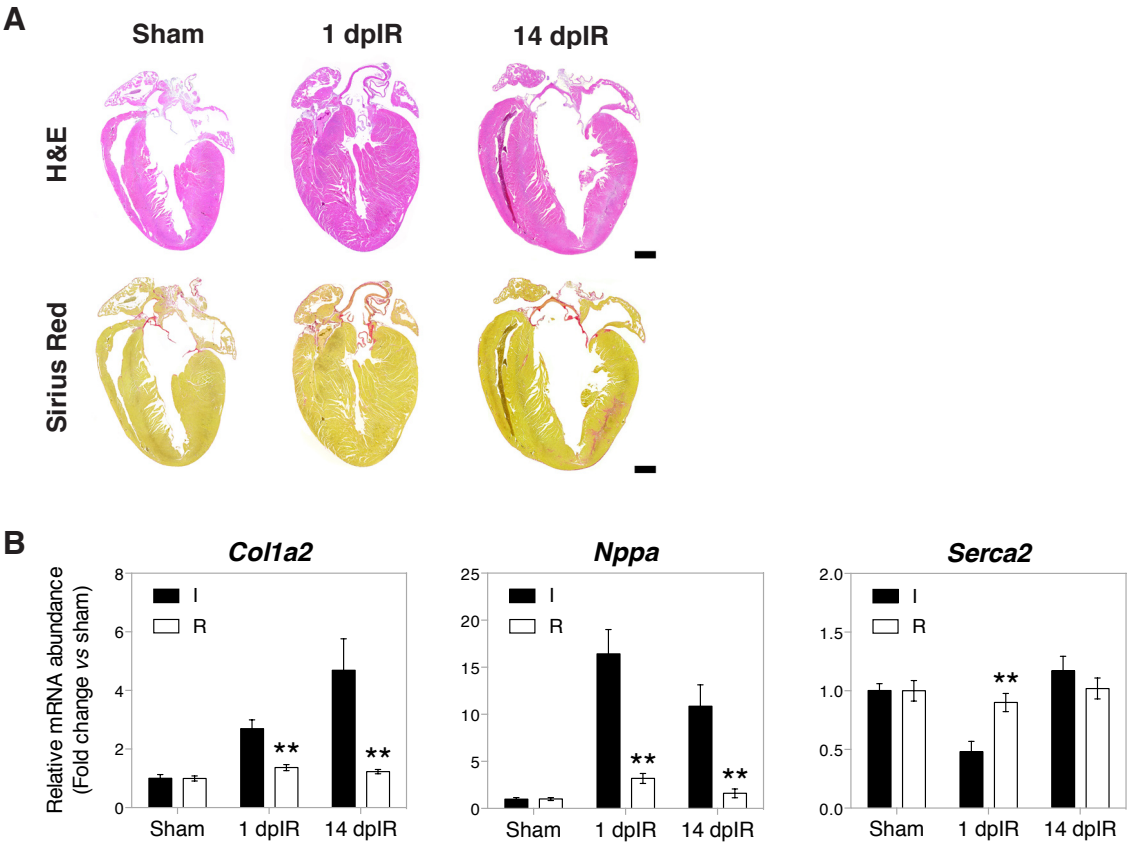

Supplemental Figure 2

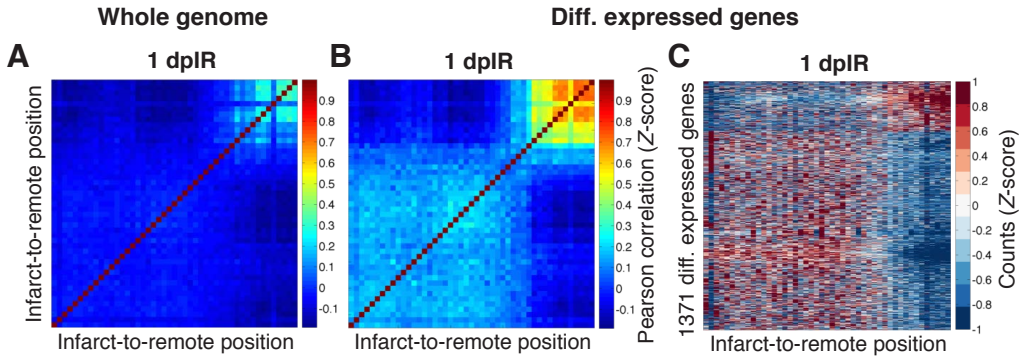

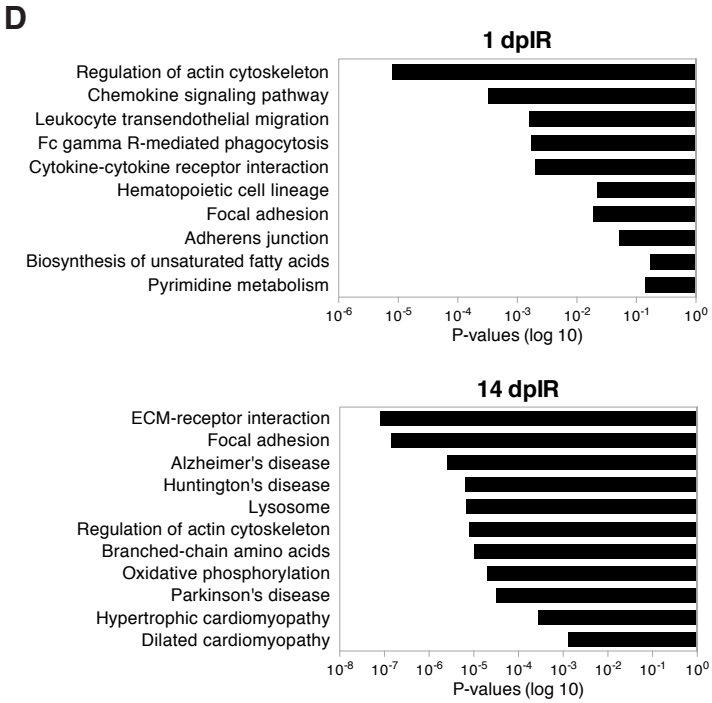

Supplemental Figure 3

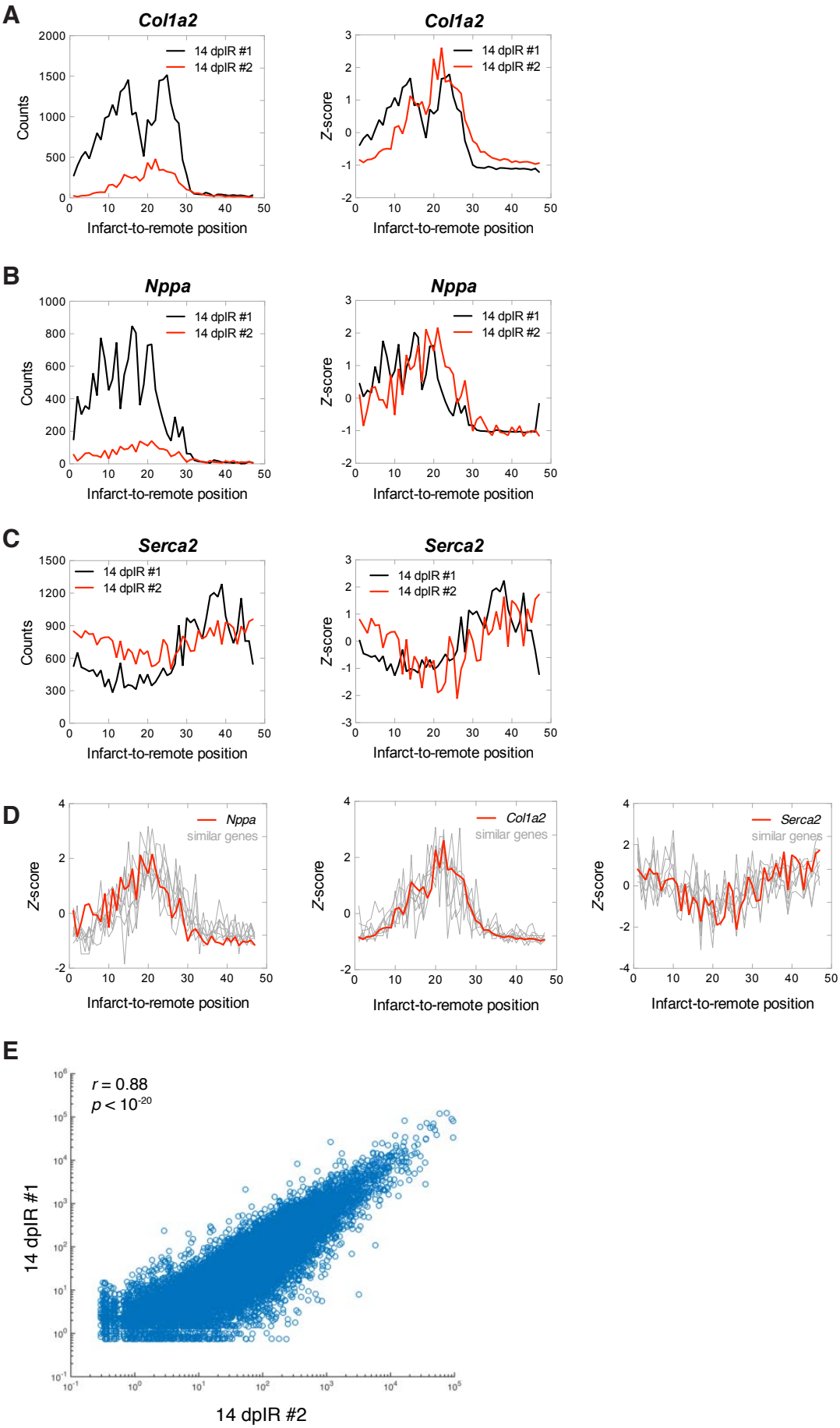

Supplemental Figure 4

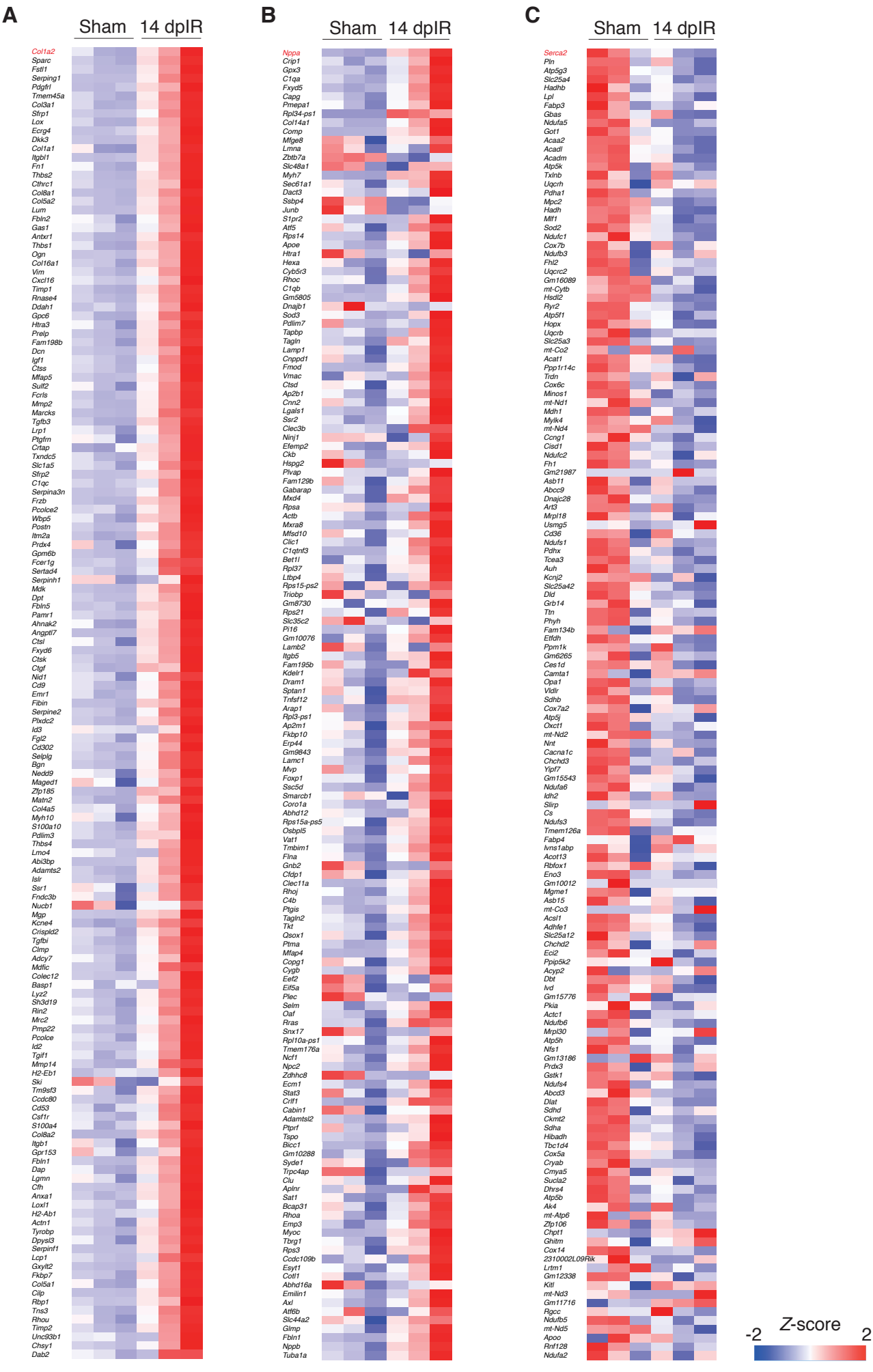

Supplemental Figure 5

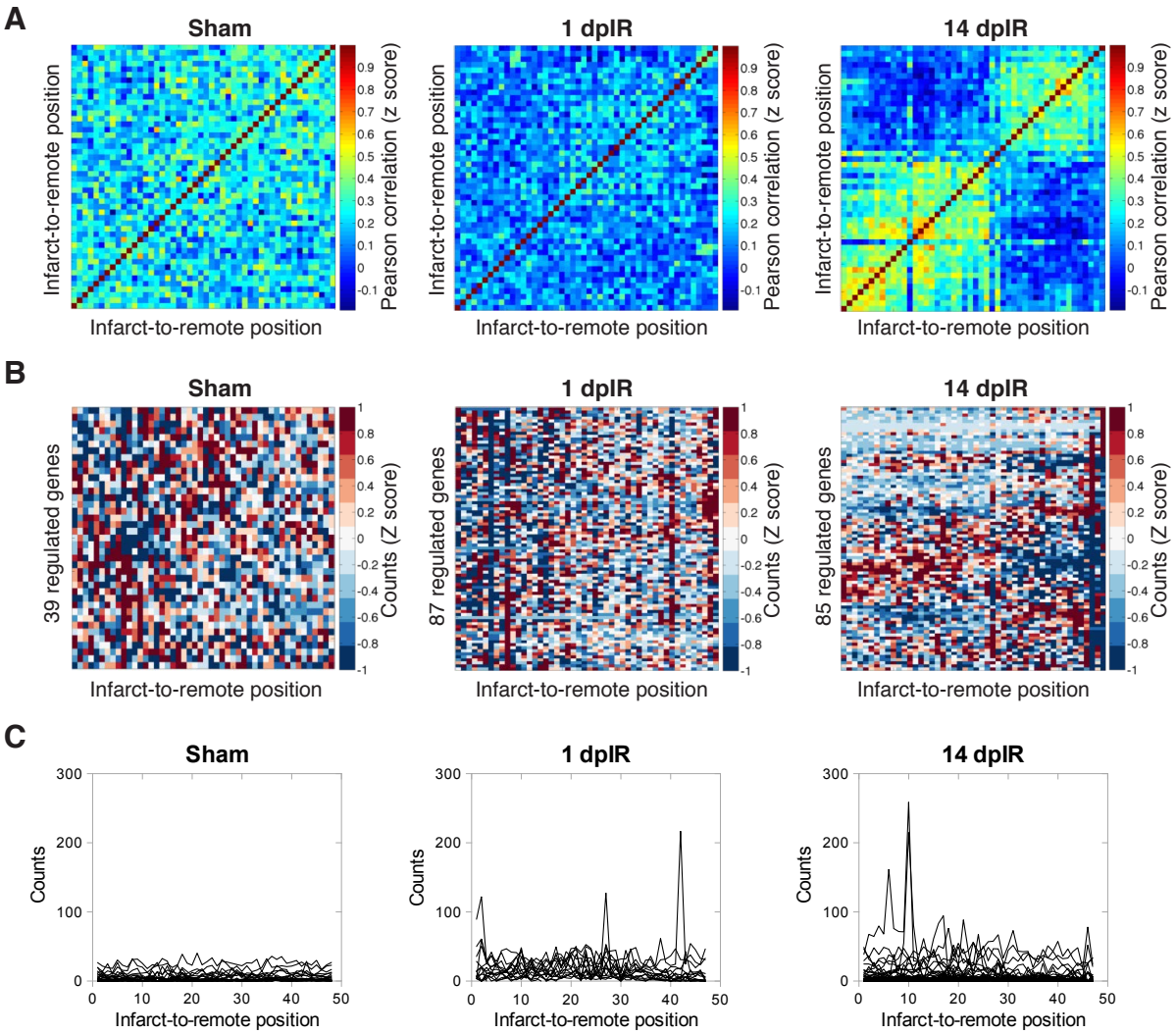

Supplemental Figure 6

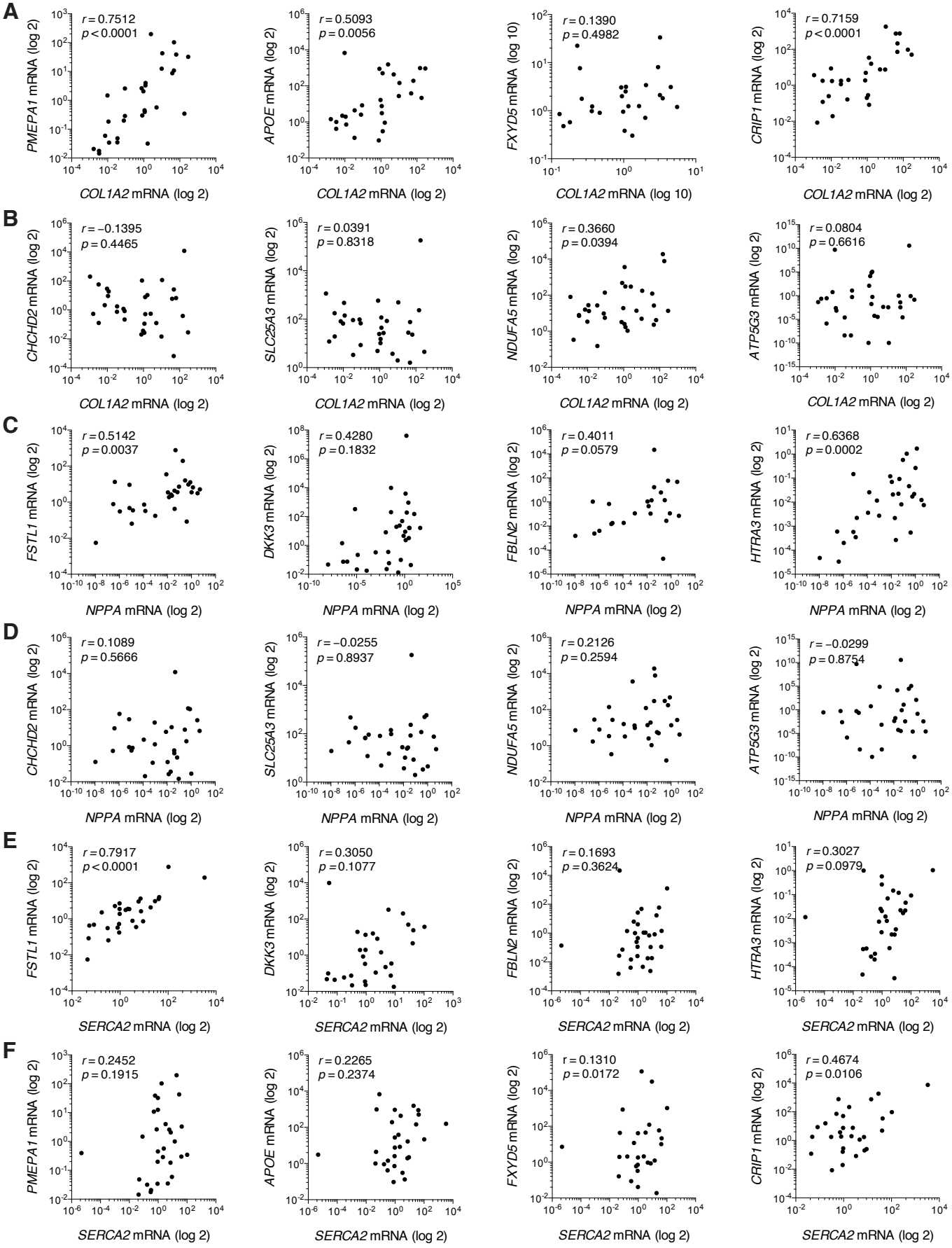

Supplemental Figure 7

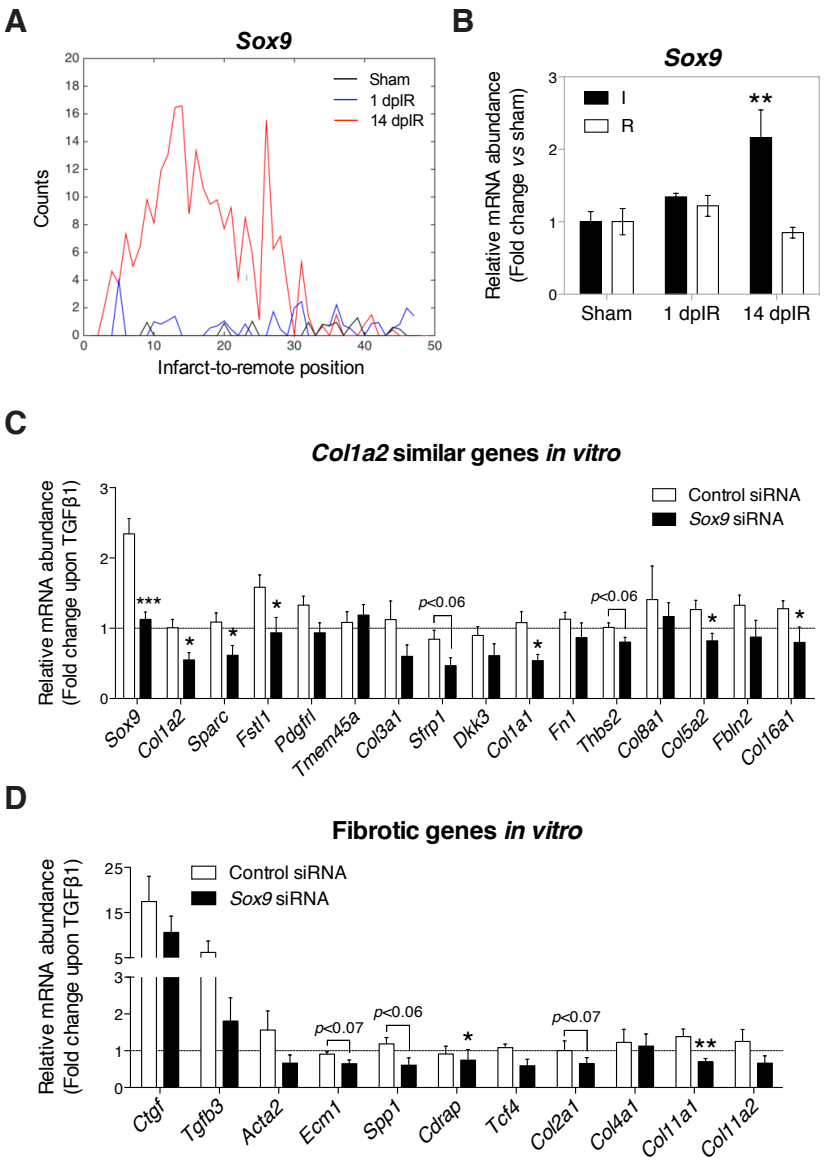

Supplemental Figure S8

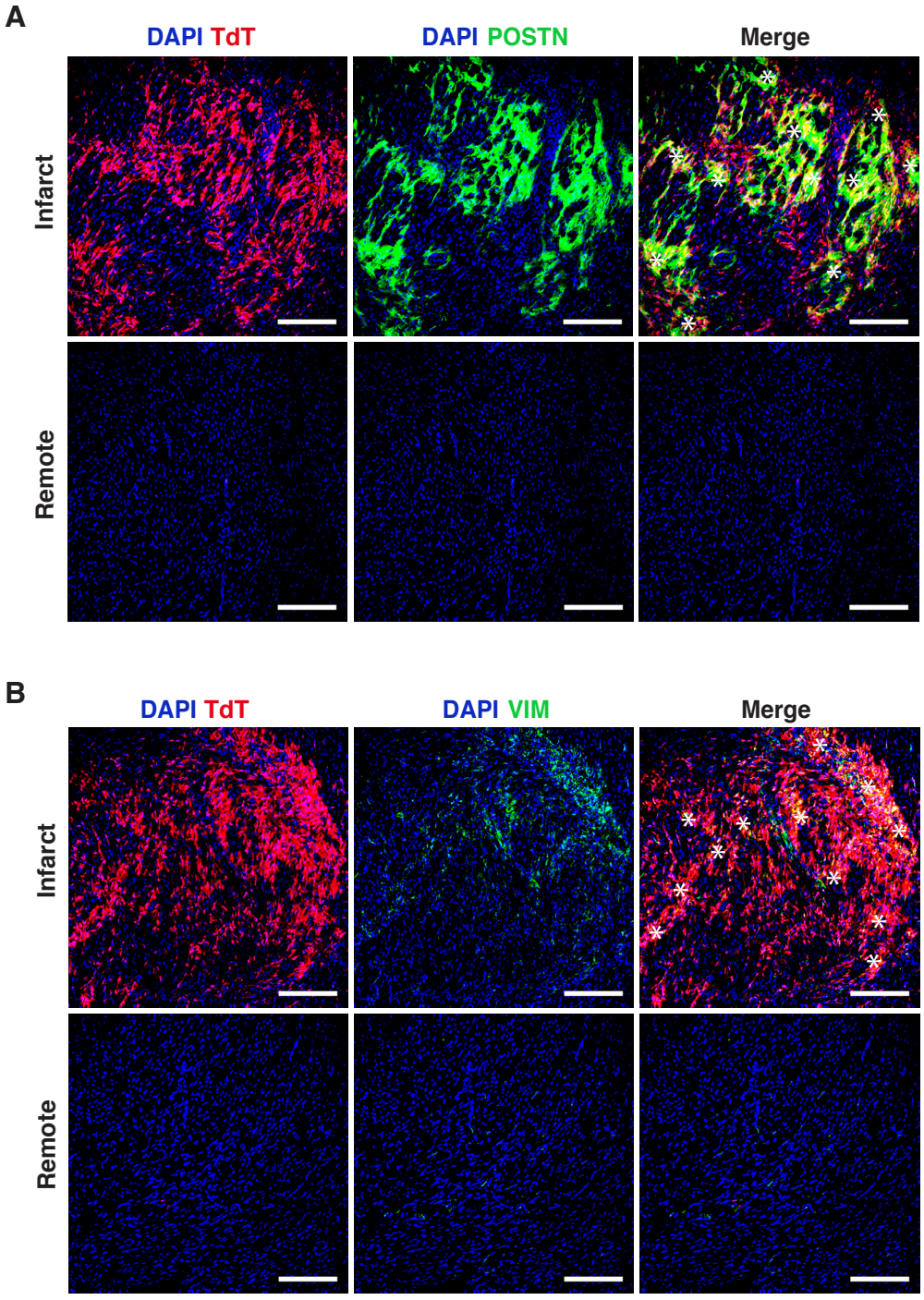

Supplemental Figure 9

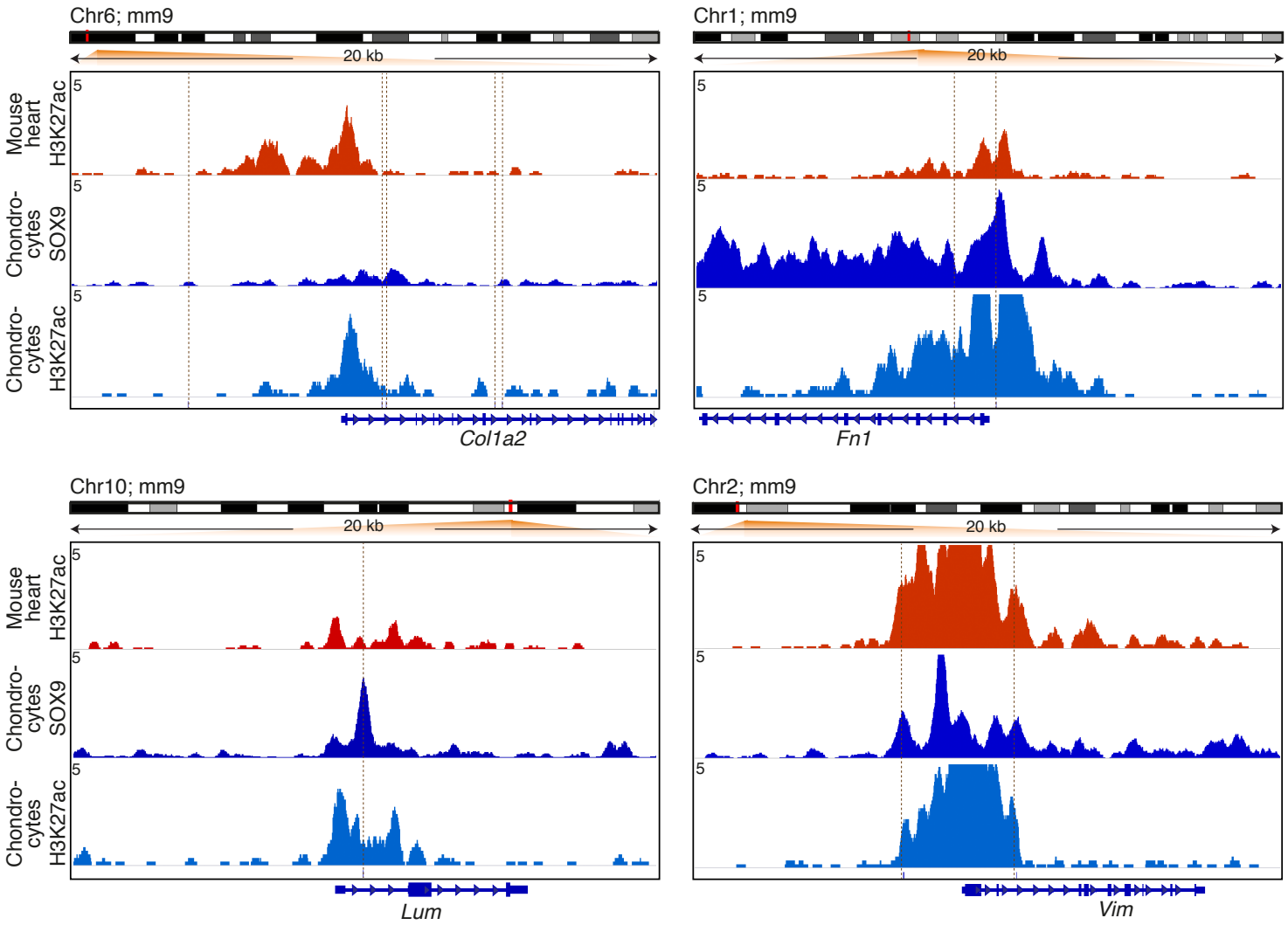

Supplemental Figure Legends

Supplemental Figure 1. Cardiac ischemia-reperfusion injury. A, Histological sections of hearts stained for Hematoxylin and Eosin (H&E) or Sirius Red from Sham, 1, and 14 dpIR mice. Scale bars, 1 mm. **B**, Real-time PCR analysis of three reference genes associated to cardiac fibrosis (*Col1a2*), remodeling (*Nppa*), and contractility/calcium handling (*Serca2*) in infarct (I) and remote (R) zones in Sham, 1, and 14 dpIR mice (n=6 per group; $^{**}p<0.01$ *vs* infarct).

Supplemental Figure 2. High resolution gene expression atlas of the infarcted heart by tomo-seq. A, Pairwise correlation for all sections across all genes expressed at >4 reads in >1 section analysed by tomo-seq 1 dpIR in one biological replicate. **B**, Pairwise correlation for all sections across genes exhibiting at least two-fold and statistically significant differential expression between the infarct and remote zones by tomo-seq at 1 dpIR. **C**, Hierarchical clustering of expression traces for all genes exhibiting at least two-fold and statistically significant differential expression between the infarct and remote zones, using Euclidean distance as metric at 1 dpIR. **D**, KEGG analysis showing the enriched pathways the genes exhibiting a two-fold differential expression between the infarct and remote zones at 1 or 14 dpIR are involved in. Pathways are ranked by their respective p value corrected by the Benjamini-Hochberg method.

Supplemental Figure 3. Confirmation of tomo-seq data. A through **C**, Spatial expression pattern of *Col1a2* (**A**), *Nppa* (**B**), and *Serca2* (**C**) determined by tomo-seq 14 dpIR in two distinct biological replicates (14 dpIR #1 and #2). Traces show gene expression as the number of read counts (*left*) or after *Z*-score normalization (*right*). *Z*-score normalization removes overall expression differences between genes by setting the mean to 0 and the standard

deviation to 1. **D**, Spatial expression traces of ten co-regulated genes 14 dpIR in the second biological replicate based on the data obtained in the first biological replicate. Reference genes are shown in red, and ten most similar genes are shown in grey. **E**, Spearman correlation between the two sets of samples. Data are shown as total number of reads (summed over all sections) for each gene.

Supplemental Figure 4. Validation of tomo-seq by RNA-seq. Validation of the differential gene expression for the one hundred thirty most similar genes to *Col1a2* (**A**), *Nppa* (**B**), and *Serca2* (**C**) between Sham and 14 dpIR hearts by RNA-seq performed on the complete injured area or a corresponding region in the Sham hearts (n=3 per group).

Supplemental Figure 5. High resolution lncRNA expression atlas of the infarcted heart by tomo-seq. A, Pairwise correlation for all sections across all non-coding genes detected at greater than four reads in more than one section by tomo-seq in the hearts from Sham, 1, and 14 dpIR mice. Especially at 14 dpIR, anatomical regions of the infarcted heart i.e., infarct and remote zones are detectable as clusters of correlated sections. **B**, Hierarchical clustering of expression traces for all genes exhibiting a peak of expression using Euclidean distance as metric. **C**, Spatial expression traces of detected non-coding genes by tomo-seq in the hearts of Sham, 1, and 14 dpIR mice. Traces are shown as read counts.

Supplemental Figure 6. Lack of correlation between genes from different reference lists. Real-time PCR analysis on human ischemic heart tissue indicating the lack of correlation when cross-referencing genes from different lists. **A**, *COL1A2* expression correlation with the expression of *NPPA* co-regulated genes. **B**, *COL1A2* expression correlation with the expression of *SERCA2* co-regulated genes. **C**, *NPPA* expression correlation with the expression of

COL1A2 co-regulated genes. **D**, *NPPA* expression correlation with the expression of *SERCA2* co-regulated genes. **E**, *SERCA2* expression correlation with the expression of *COL1A2* co-regulated genes. **F**, *SERCA2* expression correlation with the expression of *NPPA* co-regulated genes. Control hearts and remote, border-zone and infarct zones from ischemic hearts are plotted. Data are presented as log 2 transformed values. Pearson correlation (r) and significance of co-regulated gene expression is shown (n=27–34; p<0.05 is considered as significant).

Supplemental Figure 7. Regulation of ECM-related genes. A, Spatial expression pattern of *Sox9* determined by tomo-seq in the hearts from Sham, 1, and 14 dpIR mice. **B**, Real-time PCR analysis of *Sox9* in the infarct (I) and remote (R) zones in the hearts from Sham, 1, and 14 dpIR mice. Data are displayed as fold change *vs* matched Sham hearts (n=5–6 per group; **p<0.01). **C** and **D**, Real-time PCR analysis of *Col1a2* co-expressed genes and other fibrotic genes including SOX9 target genes in 3T3-L1 fibroblasts activated with TGFβ1 (5 ng/ml) for 3 hrs after knock-down of *Sox9* using a siRNA (10 nM) or a control siRNA (n=5 in two independent experiments; *p<0.05; **p<0.01; ***p<0.001 *vs* control siRNA).

Supplemental Figure 8. Lineage tracing of SOX9-expressing cells. Co-immunostaining for TdTomato (TdT) and Periostin (POSTN) (**A**) or Vimentin (VIM) (**B**) in the hearts from sham-operated mice and 14 dpIR. White stars in the Merge field indicate SOX9-TdT-positive regions. Scale bars, 200 μm.

Supplemental Figure 9. Peak intensity plots of ChIP-seq reads for SOX9 and histone modification marks (H3K27ac) in four ECM related genes induced in the heart 14 dpIR. Normalized read signals from each ChIP-seq were plotted on a 20-kb window flanking the SOX9 binding sites predicted by oPOSSUM 6.0 (cf. Supplemental Table 6). ChIP-seq signals

for H3K27Ac obtained in the heart (ENCODE dataset) were mapped to the corresponding SOX9 peak regions obtained in chondrocytes.[8]

Supplemental References

1. Junker JP, Noel ES, Guryev V, Peterson KA, Shah G, Huisken J, McMahon AP, Berezikov E, Bakkers J and van Oudenaarden A. Genome-wide RNA Tomography in the zebrafish embryo. *Cell*. 2014;159:662-675.
2. Hashimshony T, Wagner F, Sher N and Yanai I. CEL-Seq: single-cell RNA-Seq by multiplexed linear amplification. *Cell Rep*. 2012;2:666-673.
3. Li H and Durbin R. Fast and accurate long-read alignment with Burrows-Wheeler transform. *Bioinformatics*. 2010;26:589-595.
4. Huang da W, Sherman BT and Lempicki RA. Systematic and integrative analysis of large gene lists using DAVID bioinformatics resources. *Nat Protoc*. 2009;4:44-57.
5. Pritchett J, Harvey E, Athwal V, Berry A, Rowe C, Oakley F, Moles A, Mann DA, Bobola N, Sharrocks AD, Thomson BJ, Zaitoun AM, Irving WL, Guha IN, Hanley NA and Hanley KP. Osteopontin is a novel downstream target of SOX9 with diagnostic implications for progression of liver fibrosis in humans. *Hepatology*. 2012;56:1108-1116.
6. Akiyama H, Chaboissier MC, Martin JF, Schedl A and de Crombrugghe B. The transcription factor Sox9 has essential roles in successive steps of the chondrocyte differentiation pathway and is required for expression of Sox5 and Sox6. *Genes Dev*. 2002;16:2813-2828.
7. Kopp JL, Dubois CL, Schaffer AE, Hao E, Shih HP, Seymour PA, Ma J and Sander M. Sox9+ ductal cells are multipotent progenitors throughout development but do not produce new endocrine cells in the normal or injured adult pancreas. *Development*. 2011;138:653-665.
8. Ohba S, He X, Hojo H and McMahon AP. Distinct Transcriptional Programs Underlie Sox9 Regulation of the Mammalian Chondrocyte. *Cell Rep*. 2015;12:229-243.